

M. Quinten
J. Stier

Absorption of scattered light in colloidal systems of aggregated particles

Received: 28 March 1994
Accepted: 17 August 1994

M. Quinten
1. Physikalisches Institut
RWTH Aachen
52056 Aachen, FRG

J. Stier
Forschungszentrum Juelich
ICG-3 Postfach 1913
52425 Jülich, FRG

Abstract Scattering and extinction of colloidal systems containing either nonabsorbing or strongly absorbing spherical particles of some nanometers in diameter were examined in the wavelength range from the near UV to the near IR. If aggregation occurs, scattering and extinction are modified with respect to the single sphere systems. The influence of aggregation can best be recognized for absorbing particles when already the single sphere shows resonant extinction. In this case, the resonance of the single sphere splits into many new resonances for the

aggregate, most of which are positioned at larger wavelengths than the single sphere resonance. They strongly depend on the size and shape of the aggregate.

Looking at the scattering, additional problems arise in systems of absorbing particles caused by reabsorption by neighboring spheres or aggregates. A simple model was developed to interpret the obtained scattering data.

Key words Scattering – absorption – aggregates of spheres – electrolyte induced aggregation

Introduction

Light scattering and absorption by small particles has been the subject of many studies concerning fluid mechanics, photography, particle sizing, colloid science and aerosols. Clustering of particles, that is, the binding of particle aggregates, changes the optical properties of particle systems and renders the interpretation of measurements more difficult.

In this paper, we want to present experimental results on systems of aggregated spherical particles and discuss the consequences of clustering for the optical extinction and scattering of these systems.

We examined the wavelength dependence of the extinction and scattering cross-section of nonabsorbing polystyrene latex spheres and strongly absorbing silver spheres. In contrast to dielectric latex spheres, nanometer-sized silver spheres show resonant extinction in the visible spectral

region that is called surface plasmon polariton. If aggregation occurs, this single sphere resonance splits into many new resonances. This was examined theoretically by Gérardy and Ausloos [5] for small sodium particles and experimentally, for example, by Kreibig et al. [6], Fornasiero and Grieser [7], and Quinten [8] for silver and gold particles.

Looking at the measured scattered light of the absorbing silver particles there are additional problems. Although multiple scattering effects could be neglected in our experiments, the absorption of scattered light on its way to the detector influenced the spectra.

In section 1, we give the preparation method and the experimental setups. In section 2, we then give experimental results on aggregated polystyrene latex particles and silver particles. Comparisons are made with calculated spectra in section 3. The differences occurring in the scattering spectra with respect to the extinction spectra in the case of the silver particles are discussed within a simple

model, which takes into account reabsorption in the ensemble of particles.

Preparation methods and experimental setup

Preparation

It is a well established method to prepare metal particle colloids by chemical reduction of the metal from a corresponding metal salt solution.

For preparation of silver particles in aqueous solution, we used techniques of Garbowski [1] and Zsigmondy [2].

For preparation of an aqueous silver colloid after Garbowski, dissolve 0.5905 g AgNO_3 in 250 ml aqua bidi and prepare a 2%- NH_3 solution. As reducing agent prepare a tannic acid solution by solving 0.1 g tannic acid in 100 ml aqua bidi. Prepare freshly. Then mix 148 ml aqua bidi, 0.5 ml tannic acid solution, and 1 ml silver nitrate solution in a 250 ml Erlenmeyer flask and heat the mixture up to the boiling point of water. Under continuous stirring carefully add 0.5 ml of the NH_3 -solution. The reduction of Ag is completed some minutes after addition of NH_3 and the prepared colloid is yellow colored. Thereby, it is possible to obtain monodisperse spherical silver particles with mean diameters between $2R_0 = 7$ nm and 16 nm. In our experiment, we achieved a mean particle size of $2R_0 = 16$ nm.

In a next step, these particles are used as nuclei to prepare particles of larger size. This method is described by Zsigmondy in detail and can be summarized as is done in the following.

For preparation of silver particles with diameter $2R_1$, using silver particles of known diameter $2R_0$ as nuclei, the volume V_1 of required nucleus colloid is obtained from

$$V_1 = \frac{m_1}{m_0} V_0 \frac{R_0^3}{R_1^3 - R_0^3}, \quad (1)$$

where V_0 is the volume of the nucleus colloid, here $V_0 = 150$ ml, m_0 is the volume of silver nitrate solution used for preparation of the nucleus colloid, here $m_0 = 1$ ml and m_1 is the volume of silver nitrate solution used for preparation of the current colloid, here $m_1 = 1$ ml. Mix in a 250 ml Erlenmeyer flask ($75 \text{ ml} - V_1$) aqua bidi, V_1 nucleus colloid, m_1 silver nitrate solution and 1 ml NH_3 -solution. The concentrations of the AgNO_3 solution and the NH_3 -solution are the same as used for the nucleus colloid. We wanted to prepare a colloid with $2R_1 = 40$ nm, so we had to add $V_1 = 10.25$ ml nucleus colloid. Now, add aqua bidi to the mixture until the total volume is 100 ml. Prepare a 2% formaldehyde solution as reducing agent and carefully add 0.2 ml to 0.4 ml of this solution to the mixture under continuous stirring. After some minutes the

silver is completely reduced and a yellow-colored colloid is obtained. For particle sizes $2R_1 \geq 30$ nm scattering of light by the suspended particles is observable already with the naked eye.

We obtained a colloidal suspension containing nanometer-sized spherical silver particles with $2R = 36$ nm and with a standard deviation of ± 4 nm. The volume fraction was about $\phi = 10^{-6}$. (We should mention that the volume fraction is quite constant in all colloidal silver systems prepared by these means, while the mean particle size can be varied from $2R = 4$ nm to about $2R = 80$ nm).

The polystyrene latex spheres were purchased from Duke Scientific Corporation and had a mean size of $2R = 40$ nm with a standard deviation of ± 1.8 nm. The aqueous solution was diluted to a concentration of $4.56 \cdot 10^{13}$ particles/ cm^3 , which corresponds to a volume fraction $\phi = 1.5 \cdot 10^{-3}$.

Hydrosols have the advantage that particles are prevented from aggregation due to an ionic double layer around the particles. The double layer results in an electrostatic repulsion which counteracts the Van der Waals attraction among the particles. At fairly distances from the surface of a particle the repulsion dominates and the particles remain separated from each other. In addition, for very small particles the diffusive Brownian motion is much larger than the sedimentation, so the particles stay suspended in the solution for long times. On the other hand, the strength of the repulsion depends nonlinearly on the actual concentration of ions in the solution. An increase of the ion concentration lowers the repulsion and at a critical concentration the particles begin to agglomerate; after a while the particles will be removed from the solution. But the aggregation process can be stopped prior by addition of a protective colloid like, for example, gelatin, resulting in stable aggregated samples. That means that the hydrosols allow a controlled aggregation of particles. For a more detailed discussion of the stability of lyophobic colloids, we refer to, for example, Verwey and Overbeek [3].

Samples containing aggregates of spherical particles were produced by addition of small amounts of an

Table 1. Concentrations of 0.1 M Na_2CO_3 and 0.001 M CuSO_4 solution in the aggregated samples

Sample n^0	Polystyrene (Na_2CO_3)	Silver (CuSO_4)
1	9.1 E-3 M	9.9 E-6 M
2	10.7 E-3 M	11.9 E-6 M
3	13.0 E-3 M	14.8 E-6 M
4	—	19.6 E-6 M

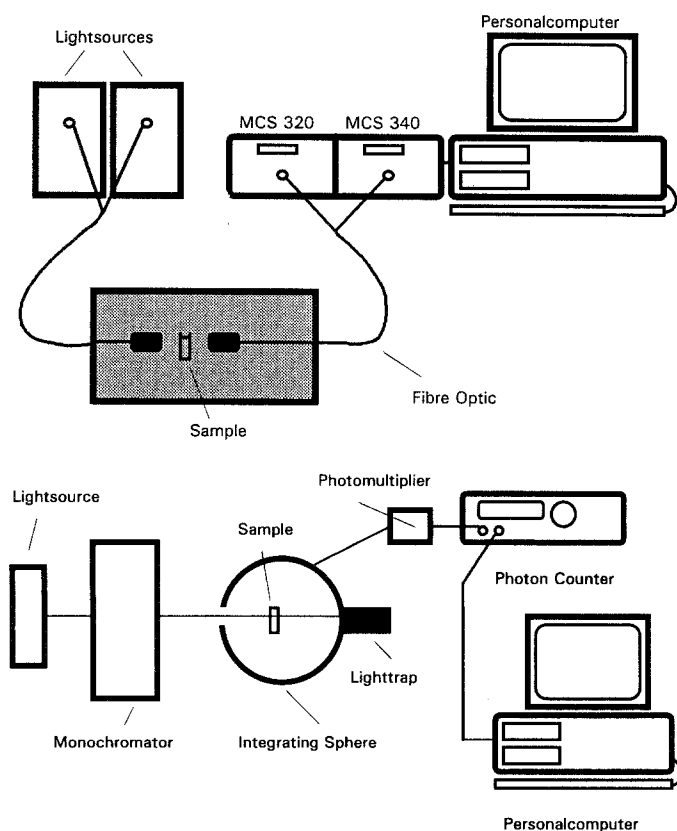
0.1 M Na_2CO_3 solution in the case of latex and of a 0.001 M CuSO_4 solution in the case of silver. Increasing the concentration of this salt solution in the suspensions, we achieved samples with different states of aggregation from the same colloid. In Table 1, we give the concentrations of the above salts in our samples.

Experimental setup

Optical extinction of the samples was measured in transmission with the experimental setup shown in Fig. 1a. With the two multichannel spectrometers the extinction at wavelengths from 200 nm to 620 nm (MCS 320) and from 620 nm to 1000 nm (MCS 340) was measured simultaneously. Actually, the two light sources provided an evaluable wavelength range from 300 nm to 1000 nm. Finally, Lambert's law or Bouguer's law gives the intensity $I(\lambda)$ of the transmitted light of vacuum wavelength λ depending on the incident light intensity $I_0(\lambda)$ and the extinction cross-section $C_{\text{ext}}(\lambda) = C_{\text{sca}}(\lambda) + C_{\text{abs}}(\lambda)$ containing absorption and scattering

$$I(\lambda) = I_0(\lambda) \exp(-C_{\text{ext}}(\lambda) \phi / V_{\text{particle}} d), \quad (2)$$

Fig. 1 a) Experimental set-up for light transmission experiments. b) Experimental set-up for light scattering experiments (modified integrating-sphere spectrometer)



where d is the thickness of the sample (here the thickness of the used cell).

Scattering of samples ($C_{\text{sca}}(\lambda)$) was measured with a modified integrating sphere spectrometer (Fig. 1b) in the wavelength range 360 nm–700 nm. Here, the scattered light of the sample at wavelength λ is collected with an integrating sphere, while the primary beam is collected in a light trap. Only the scattered light homogeneously brightens the interior of the integrating sphere, so the photomultiplier tube receives a signal proportional to the total integrated scattering. The electrical signal from the photomultiplier is counted with a photon counter.

Experimental results

In Fig. 2, we summarize the optical extinction and scattering spectra of one representative sample series for aggregated polystyrene latex spheres as well as for aggregated silver spheres. In all spectra the extinction and scattering is plotted semilogarithmically versus the vacuum wavelength. We chose this kind of presentation, because it allows to plot similar spectra in the same figure by shifting them along the ordinate by arbitrary factors. By this means the important shape information is maintained at the cost of information about the actual magnitudes.

Before we start our discussion of the measured spectra in detail, we have to point out that changes of the spectra caused by multiple scattered light could be neglected. In general, light scattered by a particle or an aggregate can be scattered twice and more by neighboring particles or aggregates. Then, a considerable portion of such multiple scattered light may be detected in transmission experiments in addition to the normally transmitted light. In this case, Lambert's law will fail. However, this effect can be neglected for low particle concentrations. In our experiments the volume fractions of suspended particles are as low that we can use Eq. (2) for the transmitted light.

In the case of nonabsorbing latex particles extinction and scattering are identical quantities ($C_{\text{abs}}(\lambda) = 0$). Therefore, we plotted in Fig. 2a only the extinction of our latex samples. Apparently, the measured spectra of the aggregated samples scarcely differ from the spectrum of single latex spheres that is plotted by the dashed line with the exception of curve 2. In curve 2 the extinction is increased at wavelengths between 300 nm and about 500 nm. At the moment, we do not have any explanation for this increase, and we also do not have any hint from electron micrographs.

Because the wavelength dependence of the scattering of aggregates and single particles of weakly absorbing materials (absorption index κ less than approximately 10^{-4}) is

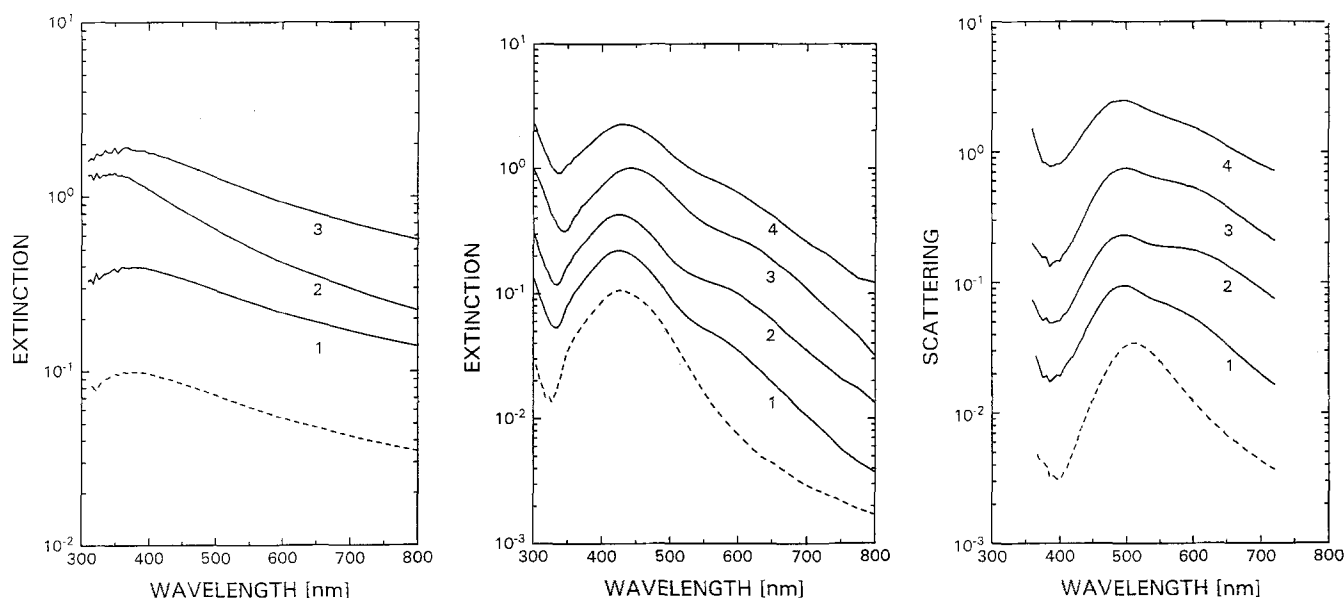


Fig. 2 Measured extinction and scattering spectra of aggregated samples. For better presentation the spectra are shifted along the ordinate by arbitrary factors. The spectra are consecutively numbered according to the approached state of aggregation. a) Polysty-

rene latex spheres, $2R = 40 \text{ nm} \pm 1.8 \text{ nm}$, extinction = scattering. b) Silver spheres, $2R = 36 \text{ nm} \pm 4 \text{ nm}$, extinction. c) Silver spheres, $2R = 36 \text{ nm} \pm 4 \text{ nm}$, scattering. The dashed line corresponds to the single particle spectrum

rather similar, it is not easy to distinguish their contributions in a mixture containing single particles and aggregates. Therefore, it has turned out for example in aerosol research to be a useful technique to introduce a mass scattering coefficient and a mass extinction coefficient, both defined as coefficient per unit mass. This takes into account that the total extinction (total scattering) is proportional to the concentration of particles of arbitrary shape that is proportional to the total mass of the particles. However, in experiments where the angular resolved scattering is measured, these quantities are not appropriate, because aggregates and single particles scatter the light in a different way (see for example ref. [9]).

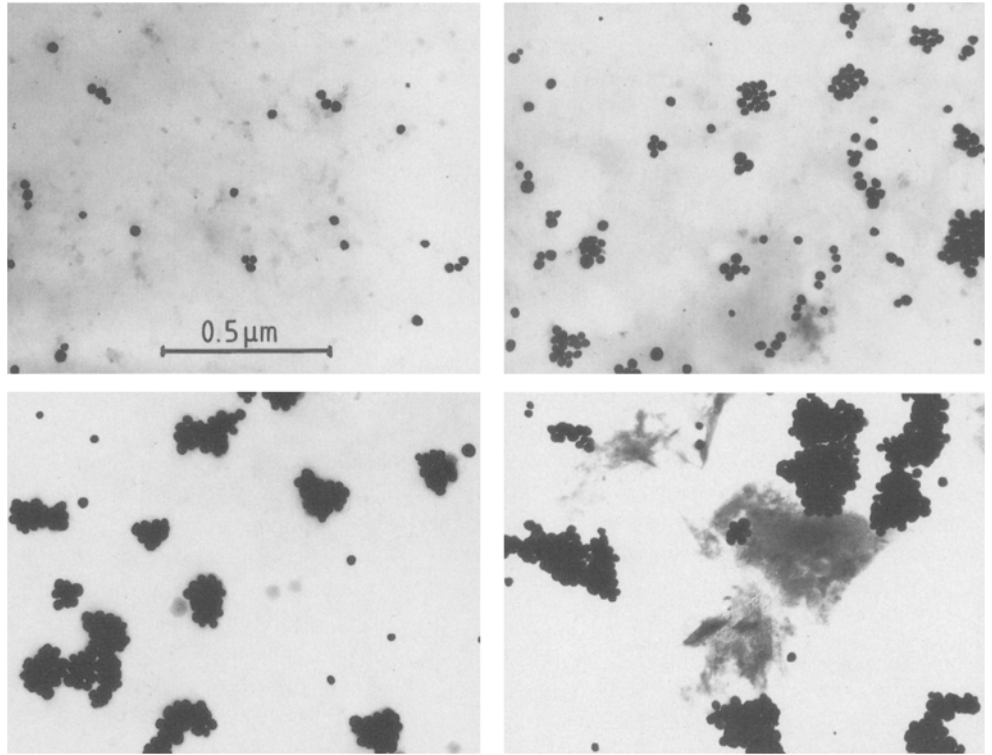
In the case of absorbing silver particles extinction and scattering are different quantities and must be measured and discussed separately. We begin here with the extinction spectra.

It becomes obvious from Fig. 2b that the spectra of the aggregated samples are quite different from the spectrum of the single spheres, plotted again as a dashed line. In particular, the single spheres show a resonant extinction band at wavelengths of blue visible light; for that reason silver colloids appear yellow-colored. This corresponds to the resonance of the dipolar TM-mode and is caused by collective excitation of the 5s-electrons in the silver particle and is called surface plasmon polariton. The extinction at still lower wavelengths in the near UV is due to excitations of interband transitions from occupied 4d levels into un-

occupied 5p levels. Additional extinction structures grow at larger wavelengths in the spectra of the aggregated samples and the low wavelength peak shifts a little bit to still lower wavelengths. These structures increase as more aggregation of particles take place. With the appearance of aggregation in colloidal silver suspensions, it can be observed that the initial color turns from yellow (single particles) to red to gray-green, depending on the state of aggregation. This is not so obvious from the presented spectra. In all aggregated samples there is a potpourri of aggregates with different shapes and sizes, as to be seen for example from Fig. 3. Then, a simple assignment of the additional peaks to a certain kind of aggregate is not possible.

Looking now in Fig. 2c at the scattering spectra of the silver sphere aggregates measured with the integrating-sphere spectrometer, one can recognize that they differ clearly from the corresponding extinction spectra. The main difference is that the peak positions of the most prominent peaks are shifted from wavelengths of about $\lambda = 420 \text{ nm} - 430 \text{ nm}$ (blue light) to wavelengths of about $\lambda = 500 \text{ nm} - 510 \text{ nm}$ (green light). Simultaneously, the intensity at wavelengths of the blue light is decreased. At wavelengths larger than about $\lambda = 530 \text{ nm}$ the shape of the spectra is similar to the corresponding extinction spectra. However, the scattered light is at least one order lower in its magnitude than the extinct light. This cannot be recognized from the figures because of the chosen

Fig. 3 Transmission electron micrographs of aggregated silver particles



semilogarithmic plot. Nevertheless, this strange and unexpected behavior is beyond any error in measurement and needs a careful explanation, as will be done in the next section.

Discussion

In this section, we want to discuss the measured extinction and scattering spectra with models.

Conclusive interpretations for the extinction spectra of spherical particles can be given with Mie's scattering theory [4]. In 1908, G. Mie gave the first complete analytical solution for the scattering and absorption of spherical particles embedded in a nonabsorbing host medium with refractive index n_M . The theory is based on the expansion of the incident wave, the scattered wave, and the wave propagating inside the sphere with vector spherical harmonics \mathbf{M}_{nm} and \mathbf{N}_{nm} into a multipolar expansion. Maxwell's boundary conditions yield relations between the unknown expansion coefficients C_{nm} , D_{nm} of the scattered wave and the known expansion coefficients A_{nm} , B_{nm} of the incident wave:

$$\begin{aligned} C_{nm} &= a_n A_{nm} \\ D_{nm} &= b_n B_{nm} \end{aligned} \quad (3)$$

a_n and b_n are the scattering coefficients of order n of

a sphere for the transverse magnetic (TM) modes and the transverse electric (TE) modes, respectively, and are given as:

$$a_n = \frac{K^2 j_n(KR) [kR j_n(kR)]' - k^2 j_n(kR) [KR j_n(KR)]'}{K^2 j_n(KR) [kR h_n(kR)]' - k^2 h_n(kR) [KR j_n(KR)]'} \quad (4)$$

$$b_n = \frac{j_n(KR) [kR j_n(kR)]' - j_n(kR) [KR j_n(KR)]'}{j_n(KR) [kR h_n(kR)]' - h_n(kR) [KR j_n(KR)]'} \quad (5)$$

where $k = 2\pi n_M/\lambda$ is the wavenumber in the host medium and $K = 2\pi(n + i\kappa)/\lambda$ is the complex wavenumber in the particle. j_n and h_n are spherical Bessel functions and spherical Hankel functions of first kind. The prime denotes the derivation with respect to the corresponding argument. We have to mention that in the case of a single sphere the symmetry of the scattering problem allows to reduce the expansions on terms with only $m = 1$. The use of the index m here provides a better comparison to the case of aggregates of spheres, as will be seen in the following.

The extinction cross-section C_{ext} and scattering cross-section C_{sca} of a single sphere are:

$$C_{\text{ext}} = 2\pi/k^2 \sum_{n=1}^{\infty} (2n+1) \text{Re}(a_n + b_n) \quad (6)$$

$$C_{\text{sca}} = 2\pi/k^2 \sum_{n=1}^{\infty} (2n+1) (|a_n|^2 + |b_n|^2) \quad (7)$$

(Re: real part).

Already in 1935, W. Trinks [10] made the first attempt to extend Mie's theory on two closely packed spheres. However, only when the additional theorems for the vector spherical harmonics were established, it was possible to extend Mie's theory on arbitrary aggregates of spheres. To our knowledge, J.M. Gérardy and M. Ausloos [5] were the first who arrived in a complete analytical description of the extinction and scattering of aggregates with arbitrary size and shape, containing N distinct spheres.

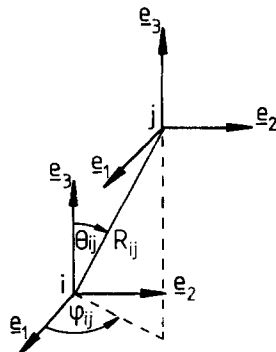
In their theory, the scattered waves of all neighboring particles are taken into account as incident waves on an arbitrary particle i with $i = 1, \dots, N$, in addition to the incident plane wave. Expanding the waves of all particles with corresponding vector spherical harmonics and using additional theorems, Maxwell's boundary conditions on the surface of the i -th sphere yield two sets of linear equations. They couple the expansion coefficients $C_{nm}(i)$, $D_{nm}(i)$ of the scattered waves with the coefficients $A_{nm}(i)$, $B_{nm}(i)$ of the incident wave:

$$C_{nm}(i) = a_n(i) \{ A_{nm}(i) + \sum_{j \neq i} \sum_{q=1}^{\infty} \sum_{p=-q}^q C_{qp}(j) S_{nmqp}(i,j) + D_{qp}(j) T_{nmqp}(i,j) \} \quad (8)$$

$$D_{nm}(i) = b_n(i) \{ B_{nm}(i) + \sum_{j \neq i} \sum_{q=1}^{\infty} \sum_{p=-q}^q D_{qp}(j) S_{nmqp}(i,j) + C_{qp}(j) T_{nmqp}(i,j) \} \quad (9)$$

We have to point out that, in this theory, it is assumed that the expansion coefficients $C_{nm}(i)$ and $D_{nm}(i)$ of the scattered waves are modified, while the scattering coefficients $a_n(i)$ and $b_n(i)$ of each particle remain unchanged. The matrix elements $S_{nmqp}(i,j)$ and $T_{nmqp}(i,j)$ depend on the spherical relative coordinates θ_{ij} , φ_{ij} and R_{ij} between particle i and j (see Fig. 4). For large distances R_{ij} they vanish rapidly and the above set of equations reduces to the single sphere case. For a more detailed discussion of the underlying theory we recommend to Gérardy and Ausloos [5].

Fig. 4 Definition of relative coordinates between two particles in a particle aggregate of arbitrary shape



The extinction and scattering cross-sections of a N -particle aggregate are:

$$C_{\text{ext}}(N) = 2\pi/k^2 \sum_{i=1}^N \sum_{n=1}^{\infty} \sum_{m=-n}^n \text{Re}(C_{nm}(i) A_{nm}^*(i) + D_{nm}(i) B_{nm}^*(i)) \quad (10)$$

$$C_{\text{sca}}(N) = 2\pi/k^2 \sum_{i=1}^N \sum_{n=1}^{\infty} \sum_{m=-n}^n |C_{nm}(i)|^2 + |D_{nm}(i)|^2 + \text{Re}\{ (A_{nm}(i) - C_{nm}(i)/a_n(i)) \times C_{nm}^*(i) + (B_{nm}(i) - D_{nm}(i)/b_n(i)) D_{nm}^*(i) \} \quad (11)$$

(the asterisk denotes the complex conjugate).

The presented theory can be applied to aggregates of arbitrary shape, size, and particle material. We used this theory to compute the extinction and scattering spectra of aggregates of polystyrene and of silver spheres. In our computations we assumed identical spheres in the aggregates. In Fig. 5, we merely give an example in which the number N of spheres in the aggregate is constant ($N = 5$), but the arrangement of the particles, which we call the shape of the aggregate, is changed. The distance R_{NN} between the centers of two neighboring particles was assumed to be $R_{NN} = 2.01 R$. In this case, the particles are closely packed but do not touch. The size of each particle was assumed to be $2R = 40$ nm, both for polystyrene and for silver. For an extensive discussion of the influence of particle size, next-neighbor distance R_{NN} and particle number N , we refer to Quinten and Kreibitz [11].

Varying the vacuum wavelength of the incoming light, we computed cross-section spectra $C_{\text{ext}}(\lambda)$ and $C_{\text{sca}}(\lambda)$ according to Eqs. (6) and (7) for the single particle and according to Eqs. (10) and (11) for the aggregates. With Eq. (2), finally, extinction and scattering spectra are obtained which are comparable to measured spectra. For the embedding medium we used the refractive index of water in the appropriate wavelength range [12] and for the silver particles the optical constants of Johnson and Christy [13].

As becomes obvious from Fig. 5a, the extinction (= scattering) of aggregated polystyrene spheres only differs slightly from each other. Moreover, there is no remarkable difference compared to the single sphere extinction. This confirms our result in Fig. 2a where the measured spectra of latex samples are plotted.

In the case of absorbing silver spheres, the TM-mode resonance of the single sphere apparently splits into many new resonances if aggregation occurs. They lead to additional extinction and scattering at larger wavelengths and strongly depend on the shape of the aggregate. The closer the aggregate is packed, the more the peak splitting of the peaks decrease. For closely packed three-dimensional aggregates that are not considered here explicitly, even the

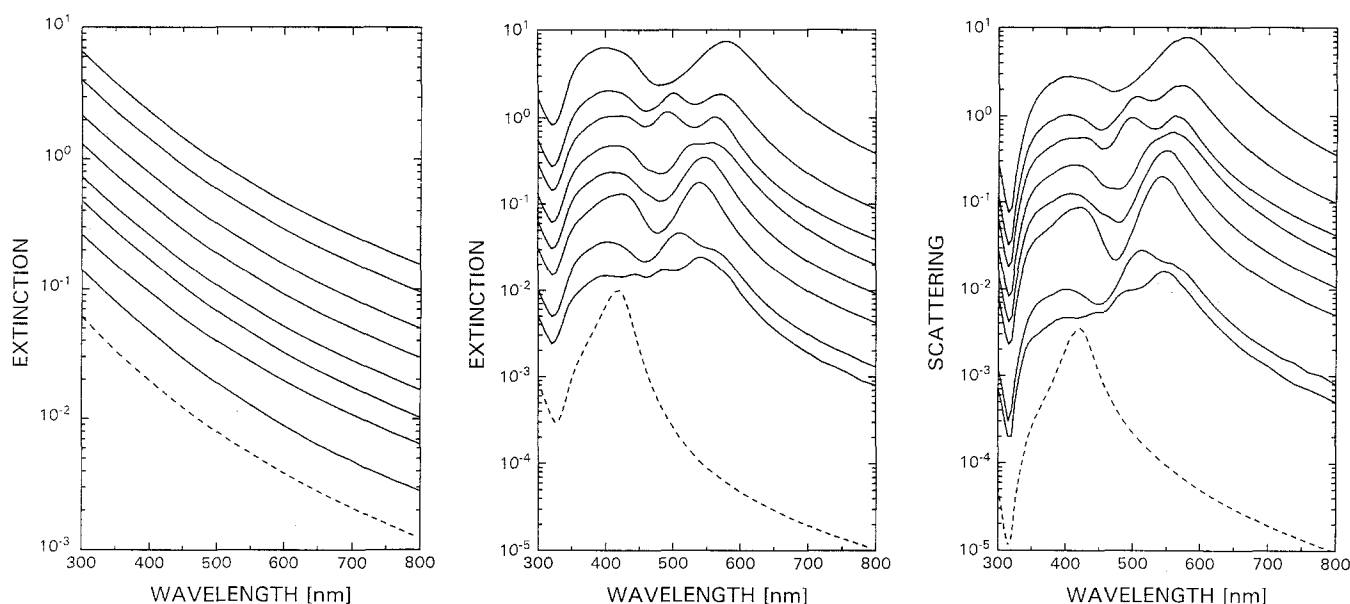
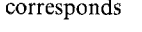


Fig. 5 Computed extinction and scattering spectra for aggregates with $N = 5$ identical spheres of $2R = 40$ nm in diameter. Again, the spectra are shifted along the ordinate by arbitrary factors. a) Polystyrene latex spheres, extinction = scattering. b) Silver spheres, extinction. c) Silver spheres, scattering. From top to bottom the spectra belong to the following particle arrangements in the aggregate: . The dashed line corresponds to the single particle spectrum

spectra can be approximated by larger spherical particles (see for example [11, 14]).

The computed extinction spectra in Fig. 5b do not completely explain the measured spectra in Fig. 2b. The reason is that in the samples, there is a potpourri of different aggregates while in our computations we only considered the example of aggregates with $N = 5$ particles per aggregate. But we can argue that the extension of Mie's theory on aggregates of spheres enables a reasonable qualitative description of the influence of aggregation on optical extinction, because we actually get an increased extinction at larger wavelengths. In detail, however, a more extended analysis of each sample by transmission electron microscopy is needed to give a complete qualitative and quantitative description of measured extinction spectra. This has been done recently for gold particle aggregates by Quinten and Kreibig [15].

Comparing the computed scattering spectra (Fig. 5c) with the measured spectra in Fig. 2c, there are remarkable differences which cannot be resolved by a detailed analysis of the samples. In our opinion, they are caused by partial absorption of the light scattered by a sphere or an aggregate by all other surrounding spheres or aggregates on its way to the detector. In the following, we want to introduce a simple model which implies this higher order extinction effect.

Consider an ensemble of spherical particles which are dispersed to low volume fraction ϕ in a transparent cell (Fig. 6). While passing through the cell of thickness d , length l and height h , the incident light will be attenuated according to Lambert's law. The following considerations are restricted on the scattering in the ensemble of absorbing and scattering spheres. At first, assume only one scattering sphere in the cell and the surrounding medium as non-absorbing. The light scattered by the single sphere into an angular element $d\Omega$ is given by the differential scattering cross-section per unit area $\partial Q_{\text{sca}}/\partial\Omega$ of the sphere as

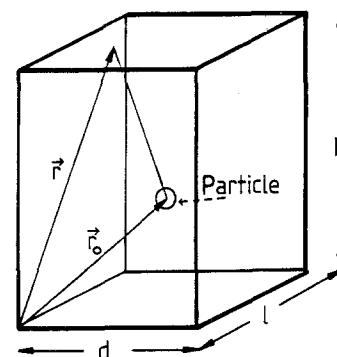
$$I_{\text{sca}}(\Omega) = \partial Q_{\text{sca}}/\partial I_0. \quad (12)$$

The integrated scattered intensity is simply

$$I_{\text{sca,det}}(1) = \int \int I_{\text{sca}}(\Omega) d\Omega = Q_{\text{sca}} I_0. \quad (13)$$

This is the intensity that is detected by the detector in the integrating-sphere spectrometer, besides an extra constant

Fig. 6 Definition of particle position and vectors in the transparent cell



factor which takes into account the ratio of the illuminated detector area and the illuminated area in the integrating sphere. $Q_{\text{sca}}(\lambda)$ is the scattering efficiency, defined as scattering cross-section $C_{\text{sca}}(\lambda)$ normalized to the geometrical cross-section πR^2 of the scattering sphere.

As a next step, assume the surrounding medium as absorbing with an absorption constant A . In this case, the intensity of the incoming light $I(r_0)$ at point r_0 , where the scatterer is situated, has already changed from I_0 into

$$I(r_0) = I_0 \exp(-A r_0 \cdot e_x), \quad (14)$$

presuming that the incident wave propagates along the x -axis.

The intensity scattered by the particle in direction Ω now decreases according to Lambert's law and is given at point \mathbf{r} as

$$I(\mathbf{r}, \Omega) = \partial Q_{\text{sca}} / \partial \Omega I(r_0) \exp(-A |\mathbf{r} - \mathbf{r}_0|), \quad (15)$$

where \mathbf{r} is the position at which the scattered light leaves the cell. Because $|\mathbf{r} - \mathbf{r}_0|$ depends on the scattering direction Ω under consideration, the detected intensity for one particle is now much more complicated

$$I_{\text{sca, det}}(1) \iint \partial Q_{\text{sca}} / \partial \Omega I(r_0) \exp(-A |\mathbf{r} - \mathbf{r}_0|) d\Omega. \quad (16)$$

In the case of an ensemble of n scattering and absorbing particles, one can sum up the contributions of all n particles, presuming multiple scattering effects can be neglected, as in our experiments. Without consideration of higher order extinction effects the integrated scattered intensity for identical spheres is then simply given by multiplication of Eq. (13) by n . On the other hand, one has to use Eq. (16) for each particle i with $i = 1, \dots, n$ with a position vector $\mathbf{r}_0(i)$ and to sum over all contributions. The absorption constant A of the embedding medium can simply be replaced by $C_{\text{ext}} \phi / V_{\text{particle}}$. To give an impression of the consequences of Eq. (16), we assume for simplicity that

- a) we can replace the angular dependent quantity $|\mathbf{r} - \mathbf{r}_0|$ by a mean constant value r_{eff} ;
- b) the extinction cross-section is dominated by the absorption cross-section, so that we can use C_{abs} instead of C_{ext} in the exponentials. (In this case, multiple scattering is neglected completely).
- c) $I(r_0)$ is replaced by I_0 .

With these simplifications the intensity of the scattered light approaching the detector is approximately given as

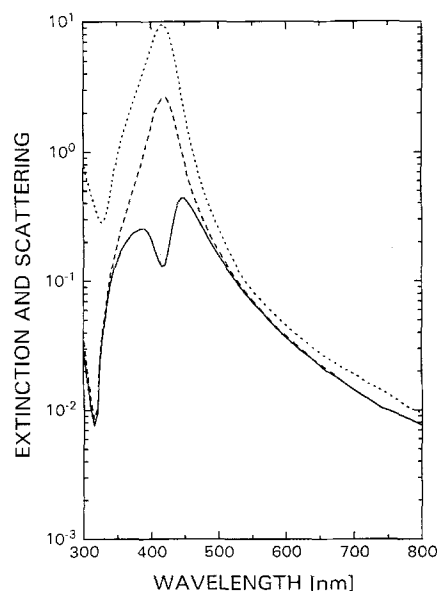
$$I_{\text{sca, det}} \approx I_0 Q_{\text{sca}} \exp(-C_{\text{abs}} \phi / V_{\text{particle}} r_{\text{eff}}). \quad (17)$$

Thus, in this approximation we expect the intensity of the scattered light to be similar to the scattered light of a single particle ($Q_{\text{sca}}(\lambda) I_0$) attenuated by the absorption by the

ensemble of particles. Note that the attenuation is wavelength-dependent due to the wavelength dependence of the absorption cross-section C_{abs} . We now compute the extinction and scattering cross sections for a single sphere according to the Mie-theory. The absorption cross-section is simply given by the difference of extinction and scattering cross-section. Using Eq. (2), we obtain the extinction spectrum shown in Fig. 7 as dotted line for a cell thickness $d = 10$ mm and a volume fraction $\phi = 10^{-6}$. According to Eq. (13), we obtain the corresponding scattering spectrum (dashed line). Finally, the higher order extinction effects are taken into account inserting extinction and scattering cross-sections into Eq. (17). The given curve in Fig. 7 (solid line) is obtained for $r_{\text{eff}} = d/2$. For better presentation, again the spectra are shifted along the ordinate by arbitrary factors. It can now be clearly recognized from this solid line that the intensity of the scattered light received by the detector is actually modified by the absorption in the colloidal suspension in such a way that it is most attenuated at wavelengths on which the particles have a large absorption cross-section. This results in an apparent shift of the maximum in the scattering spectrum to larger wavelengths.

We have to point out that the simple model of Eq. (17) only gives a reasonable qualitative description of the measured spectra, both for single spheres and for aggregates of spheres. The result shows that in the case of strongly absorbing particles the scattering spectra of a many-particle system need very careful interpretation with respect to

Fig. 7 Calculated extinction (dotted line) and integrated scattering (dashed line) of a single silver sphere in comparison with $I_{\text{sca, det}}$ (solid line) calculated using Eq. (17)



reabsorption effects. The use of a mass scattering coefficient like in aerosol research becomes questionable here.

Summary

Clustering of particles is often observed in realistic particle ensembles, for example, in colloids or in aerosols. In optical experiments such as light transmission or integrated light scattering experiments, the aggregation of particles may render the interpretation of the measured data more difficult.

In this paper, we briefly report on experiments on aggregated polystyrene spheres and silver spheres of some nanometers in diameter in aqueous solution. We chose aqueous colloids because in suspensions controlled aggregation of the single particles can be achieved easily in experiments.

In the case of nonabsorbing polystyrene particles the extinction (= scattering) spectra of aggregates scarcely differ from the scattering spectra of single spheres. Then

the scattering may be normalized to the total mass of all contributing particles, which defines a mass scattering coefficient.

Nevertheless, in the case of silver there are big differences between the spectra of single particles and aggregates. While the single spheres show a resonant extinction in the visible spectral region, the surface plasmon polariton, there are additional resonances at lower photon energies for the aggregates. They depend on the size and the shape of the aggregates. With an extension of Mie's scattering theory on arbitrary aggregates of spheres it was possible to give an explanation for the changes in the spectra.

Yet, the measured scattering spectra of aggregated silver particles deviate strongly from those calculated. The cause of this is the absorption of scattered light by all particles and aggregates in the ensemble. The mass scattering coefficient seems to fail as a characteristic quantity, if reabsorption occurs. This result holds true even if multiple scattering effects can be neglected as in our experiments.

References

1. Garbowski L (1903) *Ber Dtsch Chem Ges* 36:1215
2. Zsigmondy R (1925) *Das Kolloide Gold*, (Akademie Verlagsges., Leipzig)
3. Verwey EJW and Overbeek JTG (1948) *Theory of the Stability of Lyophobic Colloids* (Elsevier, Amsterdam)
4. Mie G (1908) *Ann Phys (Leipzig)* 25:377–455
5. Gérardy JM, Ausloos M (1982) *Phys Rev B* 25:4204–4229
6. Kreibig U, Althoff A, Pressmann H (1981) *Surface Sci* 106:308–317
7. Fornasiero D, Grieser F (1991) *J Colloid Interface Sci* 141:168–179
8. Quinten M (1989): doctoral thesis, Saarbruecken, Germany
9. Fuller KA, Kattawar GW (1988) *Optics Letters* 13:1063–1065 and 1157–1165
10. Trinks W (1935) *Ann Phys* 22:561–590
11. Quinten M, Kreibig U (1993) *Appl Opt* 32:6173–6182
12. Querry MR, Wieliczka DM, Segelstein DJ (1991) in: E.D. Palik (ed.), *Handbook of Optical Constants II*, Academic Press, San Diego, pp. 1059–1078
13. Johnson PB, Christy RW (1972) *Phys Rev B* 6:4370–4379
14. Purcell EM, Pennypacker CR (1973) *Astrophys. J.* 186: 705–714
15. Quinten M, Kreibig U (1988) in: G. Gouesbet, G. Gréhan (eds.) *Proceedings of an International Symposium on Optical Particle Sizing: Theory and Practice*, Plenum New York pp. 249–258